


 Cite this: *RSC Adv.*, 2025, 15, 7987

# Highly sensitive evanescent wave SERS probe based on exposed-core optical fibers and its application†

 Luping Meng, <sup>\*a</sup> Guangqiang Liu <sup>\*b</sup> and Zongying Feng <sup>\*c</sup>

In this study, we developed a convenient and effective method for the fabrication of evanescent wave fiber surface-enhanced Raman scattering (SERS) probes constructed with ordered silver nanocolumn arrays on the curved surface of an exposed core. An exposed core optical fiber (ECF) is a type of fiber in which the cladding is intentionally removed, providing direct access to the evanescent field of the core. Such fibers enable obtaining high evanescent field power on the core side and rapid liquid infiltration and offer a strong interaction of the evanescent wave with analytes and a long effective interaction path. Besides, the silver nanocolumn array structure coated on the curved surface of the exposed core has a larger specific surface area. Furthermore, the silver nanocolumn array structures enhance the local evanescent field surrounding the ECF to excite the target molecules and have strong light capture for the incident light, providing light-matter overlap and enhanced interaction to improve sensitivity. Such ECF SERS probes can efficiently detect 4-aminothiophenol (4-ATP) and thiram *in situ*, and a low detection limit of  $10^{-10}$  M for 4-ATP is achieved. This paper presents an easy and cost-effective technique for fabricating a highly effective and good reproducible evanescent wave fiber SERS probe, taking advantage of the synergy between manipulated ECF properties and silver nanocolumn array structures, and the probe exhibits great potential for label-free sensing and detection of biomolecules.

 Received 12th December 2024  
 Accepted 25th February 2025

DOI: 10.1039/d4ra08733j

[rsc.li/rsc-advances](https://rsc.li/rsc-advances)

## 1. Introduction

Surface-enhanced Raman scattering (SERS) is an effective method for highly sensitive, label-free detection of molecules.<sup>1–3</sup> It can even detect a single molecule in the presence of noble metals by enhancing the effective Raman scattering section.<sup>4–6</sup> Compared with normal SERS substrate platforms, SERS sensing platforms that utilize optical fibers have many advantages, including flexibility, compactness and ability for remote sensing.<sup>7–13</sup> Compared with traditional SERS substrate systems, SERS sensing platforms that utilize optical fibers offer several benefits, including their compact size, flexibility, and ability for remote detection. Consequently, optical fiber sensors have attracted extensive attention and have shown potential for applications in corrosive and harsh environments. However, the use of traditional optical fiber SERS-sensing platforms (flat-end probes) is limited by either the active region or the quantity of SERS active particles present in the region. By contrast, the evanescent wave fiber SERS probe is achieved *via* interactions between the evanescent portion of the

guided light and the analyte. Because of its larger SERS active area, this probe has been widely investigated for detecting gaseous or liquid phases.<sup>14,15</sup>

Various techniques can be used to fabricate evanescent wave fiber SERS probes using an evanescent field interaction with an analyte. For this purpose, it is common to etch the fiber to generate a tapered optical fiber.<sup>16</sup> Nevertheless, etched or tapered fibers are prone to damage and are typically fragile. Thus, the cladding of optical fibers is partially or entirely removed using either side polishing, such as D-shaped,<sup>15,17,18</sup> but the preparation process for D-shaped optical fibers results in high loss and difficulty in positioning. In addition, an exposed core optical fiber (ECF) with the side of the core exposed to the external environment can be used. The ECF was a bare core optical fiber, and it was etched optical fiber to expose the core. Such exposed core fibers are applicable for real-time sensing owing to their rapid immersion and thus a prompt response to the alteration of the surrounding environment. High sensitivity can be achieved using ECFs because of the combination of a strong evanescent field, a long fiber interaction length and a fast response of the surrounding environment. The fabrication of ECF has been experimentally verified by employing femtosecond laser micro-machining<sup>19</sup> and a focused ion beam<sup>20</sup> to expose the core or direct drawing.<sup>21</sup> However, the fabrication techniques for these configurations are complicated and require expensive equipment and a precise fabrication technology. This generally involves reducing the core diameter while also allowing for easy interaction with

<sup>a</sup>School of Optoelectronic Engineering, Zaozhuang University, Zaozhuang 277160, China. E-mail: [qfnumlp@126.com](mailto:qfnumlp@126.com)
<sup>b</sup>School of Physics and Physical Engineering, Qufu Normal University, Qufu 273100, China. E-mail: [gqliu@qfnu.edu.cn](mailto:gqliu@qfnu.edu.cn)
<sup>c</sup>School of Engineering, Qufu Normal University, Rizhao 276826, China. E-mail: [qfnufzy@126.com](mailto:qfnufzy@126.com)

 † Electronic supplementary information (ESI) available. See DOI: <https://doi.org/10.1039/d4ra08733j>


a liquid analyte. Chemical etching is a simple method for exposing the core to the external environment along the length of the core and provides direct access to the evanescent field *via* the exposed core. Some exposed-core fiber (ECF)-based sensors have recently been designed while maintaining the fiber's robustness and simple fabrication compared with other similar techniques, such as the use of tapered fibers. Wu designed a fiber evanescent wave sensor using a section of fiber where part of the cladding was removed.<sup>22</sup> They utilized HF to etch the cladding around the fiber core to obtain the sensing area, achieving the measurement of methylene blue dye at a concentration of  $10^{-7}$  mol L<sup>-1</sup>. They etched the surface of the bare core to enhance the evanescent wave interaction with the external environment. The sensitivity of the sensor is limited; simultaneously, it is still possible to improve fabrication processes.

Most recently, in our previous work, a three-dimensional (3D) fiber SERS probe was constructed using metallic nanocolumn arrays at the tip of the fiber.<sup>23</sup> This has been proven to be an easy and cost-effective method for fabricating large area ordered nano-arrays but is limited to tip-based sensing. However, very few reports in the literature have discussed the fabrication of large area ordered nano-arrays on curved surfaces. It is difficult to prepare noble metal nanoparticle structures with a large SERS enhancement factor on tapered optical fiber surfaces, so the SERS sensitivity of tapered probes is limited. Therefore, it is crucial to urgently improve detection sensitivity. Based on the above research background, we proposed a high evanescent power and high sensitivity ECF SERS probe coated with silver nanocolumn arrays on the curved surfaces of the exposed core. The longer length of the ECF provides an interaction between the sensing environment and the evanescent field and offers a significantly large region for depositing SERS active materials, which cannot be reached by end-tip fiber probes.<sup>24</sup> Coating silver nanocolumns on the curved surface of the exposed core strengthens the trapping of the evanescent wave at this interface, which leads to higher evanescent field strength, resulting in enhanced light interaction with the probe molecule. Moreover, such silver nanocolumn arrays running along the length of the exposed core are beneficial to increasing "hot spots", enhancing the interaction of guided light (evanescent field) with the probe molecule along the length of the exposed core. This contributes to the flexible butt coupling of the probe molecules with an enhanced evanescent field.

In this paper, we proposed an ECF SERS probe to detect 4-aminothiophenol (4-ATP) in real time. Such fiber SERS probes offer a powerful interaction of the evanescent field with analytes and a prolonged path of interaction. A silver nanocolumn array is deposited along the exposed core of the ECF utilizing the reactive ion etching (RIE) method while allowing the light guide to easily interact with external analytes. This provides a novel approach for the design and development of fiber SERS probes.

## 2. Fabrication and experimental setup

### 2.1 Chemical and materials

4-Aminothiophenol (4-ATP) and thiram were purchased from Sigma-Aldrich (Shanghai, China). Multimode silica fibers (105

$\mu\text{m}/125 \mu\text{m}$ ,  $62.5 \mu\text{m}/125 \mu\text{m}$ ) were purchased from Xinrui Photonics Company (China) and Corning Company (China), respectively. Milli-Q deionized water was used in all experiments.

### 2.2 Pretreatment of optical fiber

There are two major steps in the preparation of ECF SERS probes: preparation of the ECFs and fabrication of silver nanocolumn array structures on the curved surface of the ECFs. In the experiment, two fibers are used. One is a multi-mode optical fiber (MMF) with core and cladding diameters of 105 and 125  $\mu\text{m}$ ; the other is a standard single-mode optical fiber (SMF) with core and cladding diameters of 62.5 and 125  $\mu\text{m}$ , respectively. Chemical etching of such fibers results in the full exposure of the core or even thinning. To utilize the evanescent waves in the fiber, a 1.4 cm length of cladding at one end of the fiber is eliminated through chemical etching and employed as the sensing area. The fiber utilized in the current experiment is 20 cm long. At one end of the fiber, a 1.4 cm outer plastic jacket is initially removed. After the removal of the plastic jacket, the fiber was delicately washed in distilled water, allowed to dry for some time, and then dipped in 40% HF solution, in which HF was used to strip away cladding from a 1.4 cm segment of fiber, thereby exposing its core surface for use as the sensing area. The depth of the HF etched can be precisely controlled by controlling the etching time. Therefore, various probes with different core diameters were created by controlling the etching time. Four different ECFs were fabricated with different core diameters of 85.88  $\mu\text{m}$ , 57.06  $\mu\text{m}$ , 36.55  $\mu\text{m}$ , and 10.32  $\mu\text{m}$  by etching the fibers with HF for 10, 20, 30 and 40 minutes, respectively. The length of forming a rough surface on the exposed fiber core can be up to 1.4 cm. The cladding and jacket of the fiber are removed from the sensing part, thus enabling the interaction between the light within the fiber and the surrounding medium. The ECFs can provide a curved and large surface for the fabrication of silver nanocolumn array structures and the interaction of light matter.

### 2.3 Fabrication of silver nanocolumn array structures on the curved surface of an ECF

The colloidal nanosphere self-assembly combined with RIE technology was employed to prepare the ECF SERS probes. Before fabricating the silver nanocolumn on the curved surface of the exposed core, the prepared fibers were washed several times using distilled water and ethanol to remove excess HF from the surface and then dried in an air oven at 60 °C. Then, the fiber is fixed on a glass slide and cleaned with plasma cleaning for three minutes to make the curved surface of the exposed core hydrophilic. Subsequently, the self-assembly of the PS spheres method was adopted to deposit the PS spheres onto the curved surface of the exposed core. First, a layer of self-assembled arranged monolayer PS sphere was transferred to the surface of ultrapure water in the beaker. The ECF was clamped with a lifting instrument and immersed horizontally in the beaker. Then, it is lifted out of the PS sphere monolayer membrane at a certain speed. In the contact part between the PS



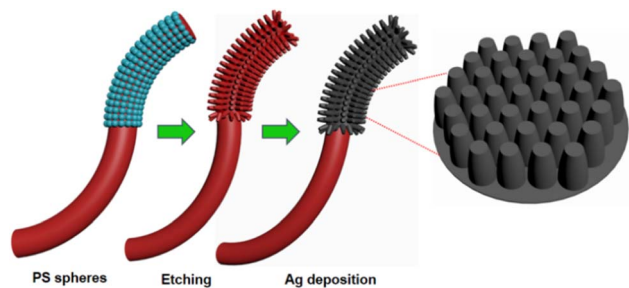


Fig. 1 A fabrication schematic for the ECF coated with silver nanocolumn arrays.

sphere suspension solution and the exposed core of the ECF, the PS sphere monolayer concentrates on the exposed core-cured surface of the fiber through surface force. A monolayer PS sphere membrane is formed onto the curved and rough surface of the exposed core. When the solvent in a monolayer PS sphere membrane volatilizes naturally, the adhesion of PS spheres is strengthened, coating the exposed core surface with a uniform self-assembled polystyrene sphere arrangement.

After that, silver nanocolumns were fabricated directly on the exposed section of the ECF by applying the RIE method. RIE was performed in plasma using  $\text{SF}_6$  with a flow rate of 80 sccm, with a pressure set to 3.2 Pa and a power of 200 W. The PS spheres coated with ECFs, with diameters of 500 nm and 1000 nm, were subjected to etching at different times, specifically 140 s and 220 s. This way achieves the uniform, stable and large surface area nanocolumn array on the curved surface of the exposed core. Finally, the nanocolumn array is coated with a (20–40 nm) silver layer, which can be performed by applying a magnetron sputtering instrument (Emitech k550x). The whole experimental process of making silver nanocolumn array structures on the curved surface of the exposed core is shown in Fig. 1. The fiber is ready for characterization and experiment.

## 2.4 Characterizations

The surface morphology of silver nanocolumn array structures on the curved surface of evanescent wave fiber SERS probes and ECF was observed and analyzed by applying a field emission scanning electron microscope (FESEM, Sigma 500).

## 2.5 SERS measurement

4-ATP ethanol solutions and thiram aqueous solutions with various solution concentrations were used to analyze the performance of the ECF SERS probes. The enhanced Raman signals that are backscattered are collected and analyzed simultaneously using a bifurcated fiber-optic module and a portable Raman spectrometer. We adopt the dip-in optical fiber method for detection. The SERS signals are recorded when the Raman excitation power is 7 mW and the integration duration is 2 s. The laser light used for excitation, with a wavelength of 785 nm, is introduced into one end of the fiber core. The Raman signal backscattered is gathered from the same end where it was launched, as illustrated in Fig. 2.

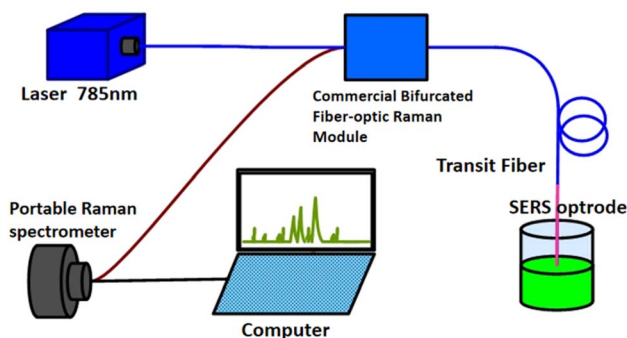


Fig. 2 Schematic for back scattered SERS measurements of the setup.

## 3. Results and discussion

### 3.1 Characterization of curved surface microstructures of an ECF

In the HF etching process, the resulting fiber core diameter gradually decreased with increased etching time. The fiber has an outer diameter of 105  $\mu\text{m}$  and effective core diameters of 85.88  $\mu\text{m}$ , 57.06  $\mu\text{m}$ , 36.55  $\mu\text{m}$  and 10.32  $\mu\text{m}$ , as shown in Fig. 3(a)–(d).

Fig. 4(a) shows the FESEM panoramic image of the evanescent wave fiber SERS probe. The uniform and highly ordered nanocolumn adhered to almost the entire curved surface of the exposed core. Fig. 4(b) shows an enlarged SEM image of the evanescent wave fiber SERS probe; a large area of the nanocolumn array structure can be observed. To further investigate the morphology and microstructure of the nanocolumn, FESEM analysis of the size of the nanocolumn (500 nm and 1000 nm) was conducted at different magnifications, as depicted in Fig. 4(c) and (d). As shown in the inset of Fig. 4(c), local magnification revealed that the height and diameter of each nanocolumn are about 500 nm and 445 nm, respectively, and the gap of two adjacent nanocolumns is approximately 55 nm. Thus, the period of the nanocolumn array structures can be controlled by changing the diameters of the PS sphere and

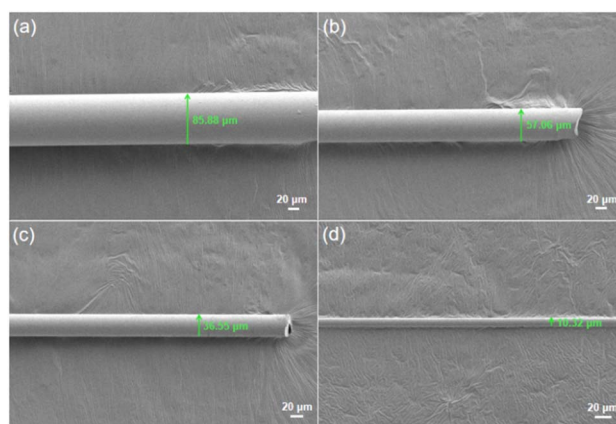


Fig. 3 FESEM image of the ECF with different diameters and HF etching times: (a) 10 min; (b) 20 min; (c) 30 min; (d) 40 min.



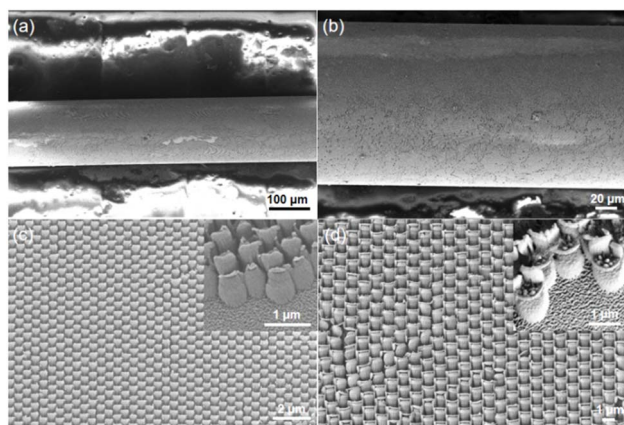


Fig. 4 Evanescent wave fiber SERS probe FESEM image: (a) panoramic view of the ECF coated with 500 nm polystyrene spheres; (b) high magnification SEM image of the ECF coated with 500 nm polystyrene spheres; (c) 500 nm silver nanocolumn arrays as a mask; (d) 1000 nm silver nanocolumn as a mask.

adjusting the etching time. A detailed description of the process of fabricating a nanocolumn array by reactive ion etching and the formation mechanism was given in our previous work.<sup>23</sup>

### 3.2 Performance of SERS

**3.2.1 Mechanism of ECF SERS probes.** For the ECF probes, the SERS interaction based on evanescent wave occurs.<sup>25</sup> We used optical fiber sensing technology and the principle of evanescent wave detection to detect active molecules within the detection range of evanescent waves in the solution, as shown in Fig. 5(a). When the excitation laser transmits in an ECF, partial energy leaks as an evanescent wave and excites the LSPR of nanoparticles on the surface. If the active molecules are just located in the SERS hotspot area provided by nanoparticles, they generate light scattering after being excited with the Raman signals enhanced greatly. The excited SERS signals are coupled back to the core and propagate through total reflection for spectral detection.

Owing to the relatively small intensity of the evanescent wave, which is only limited to the surface of the side of the fiber core, the scattering signal intensity of the active molecules

excited by the evanescent field is relatively small. On the one hand, the power of the evanescent light can be enhanced simply by reducing the core size. Moreover, when using the appropriate core size of the ECF to enhance the generated Raman scattering, the nanocolumn arrays were fabricated on the side of the fiber core by applying the RIE method, and the position was where the evanescent field was generated. Through the surface plasmon resonance between the evanescent field and the nanocolumn arrays to generate an enhanced local field as the excitation field, we can obtain the enhanced Raman scattering signal of the sample. Owing to the size of the silver nanocolumn arrays being much smaller than the attenuation depth of the evanescent wave, the evanescent wave can easily penetrate the silver nanocolumn arrays and reach the detected solution. Simultaneously, this enhancement effect depends on the size of the nanocolumn arrays and the properties of the surrounding medium. Low concentration samples can be detected using the ECF SERS probe with this technology, which also improves the detection limit and sensitivity.

**3.2.2 SERS activities for the ECF SERS probe.** To investigate the SERS performance of such an ECF SERS probe, measurements were performed in the liquid phase. The SERS measurements were conducted by immersing the exposed core (sensing region) in the sample, and detection was performed on the evanescent field generated on the surface of the exposed fiber core. The ECF SERS probe was placed inside a container containing the liquid analyte, staying in direct contact with the liquid analyte. The 4-ATP molecule functions as the signal emitter in our design; it is excited and emits SERS signals in the evanescent field.

Besides, coating silver nanocolumn arrays on the curved optical fiber surface of the ECF enhances the trapping of the evanescent wave at this interface, leading to higher evanescent field strength. Therefore, the size of the coating silver nanocolumn also affects the evanescent field strength. The effects of the size of the nanocolumn on the SERS intensity were described in our previous research.<sup>23</sup> The lateral surface area of the nanocolumn created with 500 nm PS spheres doubles that of the one formed by 1000 nm PS spheres. Therefore, we preferred 500 nm PS spheres in this experiment.

Then, we explored the influence of silver layer thickness on the SERS intensity by adjusting the silver film thickness. Prior to identifying the 4-ATP molecule, we captured the background Raman spectrum produced by the optical fiber, as illustrated in Fig. 5(b) (bottom curve). To track changes in Raman intensities, in the subsequent SERS detection experiments, all SERS spectral data were acquired by removing the background Raman signal from the fiber. The measured Raman spectra of  $10^{-6}$  M 4-ATP are displayed in Fig. 5(b) for nanocolumns with different silver layer thicknesses, ranging from 27 nm, 30 nm to 33 nm. The SERS spectra were recorded after immersing the ECF SERS probe in the sample for 10 min. Characteristic Raman peaks of 4-ATP can be detected at approximately 1079, 1187, 1180, 1347, 1495 and 1587  $\text{cm}^{-1}$ , and this aligns with earlier findings regarding the Raman peak wave number.<sup>23,24</sup> Considering the peak strength, 30 nm is the optimized silver layer thickness for the ECF SERS probe. Thus, when performing experiments, we

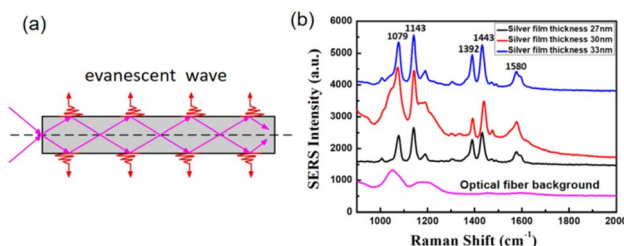


Fig. 5 (a) Evanescent field in optical fibers. (b) SERS spectra of the evanescent wave fiber SERS probe with 500 nm polystyrene spheres deposited with 27 nm, 30 nm and 33 nm silver film thicknesses to detect in 4-ATP solutions with a concentration of  $10^{-6}$  M and optical fiber background Raman spectrum.



can adjust the silver layer thickness to the optimal value of 30 nm.

We investigated the effects of different factors on the ECF SERS probe performance. Obviously, the SERS performance of the probes is affected by the intensity of the evanescent wave and the sensing length of the exposed core. First, we optimize the core diameters of ECFs to attain strong SERS interactions. To compare the sensitivity of probes with various core diameters, ECF SERS probes with different core diameters (ranging from 10.32  $\mu\text{m}$  to 57.06  $\mu\text{m}$ ) were prepared at different HF etching times and used to measure the SERS spectra of  $10^{-6}$  M 4-ATP solution. As shown in Fig. 6(a), the core diameter of the ECF directly affects the SERS performance of the ECF SERS probe. The SERS intensity of the Raman peak of  $1079\text{ cm}^{-1}$  was extracted, as shown in Fig. 6(b). As the core diameter increases, the SERS signal intensity of the probe shows a trend of first increasing and then decreasing. For probes with a core diameter of 36.55  $\mu\text{m}$ , the SERS signal intensity reaches its maximum. Smaller core fibers have been experimentally shown to provide higher sensitivity. This is because the core of the ECF functions as a micron-scaled waveguide, allowing a considerable amount of transmitted light to diffuse into the exposed side of the core in the form of an evanescent field. As the diameter of the ECF core is further minimized, there is an increase in the evanescent field strength. However, the ECF core diameter is not the thinner the better. A further decrease in ECF core diameter can remarkably increase transmission loss of the ECF<sup>26</sup> and fabrication time of the HF etching process. The core diameter was too small, such as the 10.32  $\mu\text{m}$  core, resulting in a low coupling efficiency and, as a consequence, low sensitivity (Fig. 6(a)). For this reason, the appropriate core diameter is adjusted to maximize the power collected from the fiber core. Therefore, the optimized core diameter of the ECF SERS probe

is 36.55  $\mu\text{m}$  to balance preparation time, transmission loss and evanescent wave intensity. Thus, to improve the sensitivity again, it is ideal to fabricate an ECF SERS probe with a core diameter of 36.55  $\mu\text{m}$ .

Next, we explored the effect of the sensing lengths of the exposed core of the ECF SERS probe on the SERS signal intensities. The effect of sensing length was studied by processing the sensing area of the fiber into different lengths. The sensitivity of the ECF SERS probe increases with increasing exposed core length. Experiments were performed for three different sensing lengths (0.4 cm, 1 cm and 1.4 cm) (Fig. 6(c)). By monitoring the variations in Raman intensities at the  $1079\text{ cm}^{-1}$  window, it is evident from Fig. 6(d) that there is a rapid increase in intensity with longer sensing lengths. The experimental results show that SERS intensities have a close relationship with sensing length; the longer sensing length achieved higher intensities. This can be explained by the fact that the sample molecule was infiltrated into the silver nanocolumn array and the space between them. With the increase in sensing length, the surface silver nanocolumn arrays increase, the surface area increases and the interaction on the ECF increases, which can provide a large amount of SERS "hot spots" and also enable the absorption of more probe molecules.

In this study, a core length of 1.4 cm was employed. Fig. 7(a) presents the SERS spectra of 4-ATP in concentrations ranging from  $1.0 \times 10^{-6}$  to  $1.0 \times 10^{-10}$  M. The intensity of the 4-ATP's peak diminishes as its concentration decreases, and this is due to a reduction in the number of molecules present. The limit of detection is achieved as  $1.0 \times 10^{-10}$  M. In addition, we compared our probes with recently reported ones. It is obvious that the LOD of our ECF SERS probe was lower than that of reported tapered<sup>15,21</sup> and flat-end<sup>9,10</sup> optical fiber SERS probes by at least an order of magnitude. The remarkable sensitivity of the ECF SERS probe is attributed to the significantly improved light matter interactions facilitated by the high evanescent field

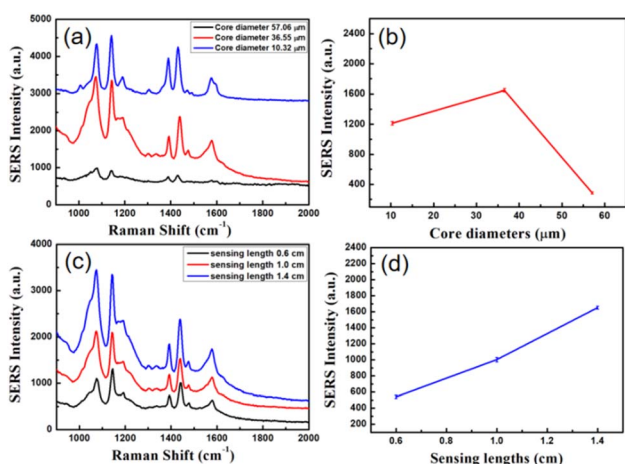


Fig. 6 (a) SERS spectra of  $10^{-6}$  M 4-ATP solutions measured using evanescent wave fiber SERS probes fabricated with different core diameters of ECFs. (b) Relationship between SERS intensity for the peak at  $1079\text{ cm}^{-1}$  and core diameters. (c) SERS spectra for  $10^{-6}$  M 4-ATP solutions measured using probes with different sensing lengths of ECFs. (d) Relation between the SERS intensity of the peak at  $1079\text{ cm}^{-1}$  and sensing lengths.

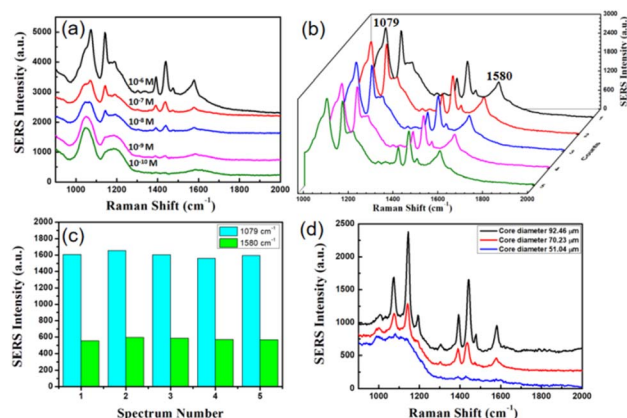


Fig. 7 (a) SERS spectra of 4-ATP solutions with concentrations of  $10^{-6}$  to  $10^{-10}$  M, obtained with evanescent wave fiber SERS probes; (b) SERS spectra of 4-ATP solutions with a concentration of  $10^{-6}$  M measured using 5 probes prepared under same process; (c) SERS intensities for peaks at  $1079\text{ cm}^{-1}$  and  $1580\text{ cm}^{-1}$ ; (d) Raman signal of the evanescent wave fiber SERS probes of different core diameters submerged in  $10^{-6}$  M 4-ATP solution.



present in active sensing regions adjacent to the liquid-filled core, as well as an enlarged area for SERS interaction due to silver nanocolumn arrays on the curved surface of the ECF. This low detection limit is attributed to a larger SERS interaction area and the SERS interactions between the ECF and the silver nanocolumn array structure. Moreover, the 4-ATP concentration is a linear kind of dependence on Raman intensity. Thus, ECF SERS probes have important applications in *in situ* liquid-phase detections.

Repeatability is an essential indicator of sensors, and it is of great significance in detecting the repeatability of the sensor. To evaluate the SERS performance of the ECF probes, five probes were repeatedly fabricated under the same conditions as the core length of 1.4 cm. The results for the reproducibility of the SERS spectrum with  $10^{-6}$  mol L $^{-1}$  4-ATP measured with the five ECF SERS probes are shown in Fig. 7(b). The SERS intensity of the Raman peak at  $1079$  cm $^{-1}$  was extracted for each measurement. The results are shown in Fig. 7(c). The relative standard deviation (RSD) for the peak was 2.1%, proving that the prepared probe has good repeatability. The experimental results also indicate that the proposed sensor possesses outstanding stability, as shown in Fig. S1.†

All the aforementioned results demonstrate that the ECF SERS probe exhibits high sensitivity, linearity, rapid response, and good repeatability. We may conclude that the ECF SERS probe has great potential in numerous sensing applications for remote measurements and has a great future.

Furthermore, the experiment utilized a single-mode silica optical fiber featuring a core diameter of  $62.5$   $\mu\text{m}$  and a cladding diameter of  $125$   $\mu\text{m}$ . We prepared different core diameters of the ECF SERS probe (ranging from  $10.32$   $\mu\text{m}$  to  $85.88$   $\mu\text{m}$ ) through different HF etching times with this fiber. Fig. 7(d) shows the SERS performance of ECF SERS probes with varying core diameters. Such fiber features a large cladding diameter ( $125$   $\mu\text{m}$ ) paired with a small core ( $62.5$   $\mu\text{m}$ ), which can be reduced even more through HF etching to enhance sensitivity. This approach allows for improved sensitivity without necessitating the direct fabrication of an ECF with a smaller core diameter. However, manipulating such thin fibers poses challenges owing to their potential impact on fiber strength.

### 3.3 FDTD simulation and theoretical calculations

The high sensitivity of the ECF SERS probe is primarily attributed to its elevated SERS EF for the silver nanocolumn array structure on the curved surface of the exposed core. Fig. 8 shows the simulated electric field intensity distribution using the finite difference time domain (FDTD) method. For this simulation, three silver nanocolumns with diameters of  $500$  nm and spaced  $50$  nm apart were modeled to analyze both the electric field distribution and the EF.

The wavelength used for excitation is  $785$  nm, and the orientation of the incident light is along the exposed core. Fig. 8(a) shows that the maximal local electric field enhancement factor  $|E_{\text{loc}}/E_0|$  is 32 for the interior of silver nanocolumns. The EF was determined using the standard formula  $|E_{\text{loc}}/E_0|^4$ , where  $E_{\text{loc}}$  represents the local maximum electric field and  $E_0$

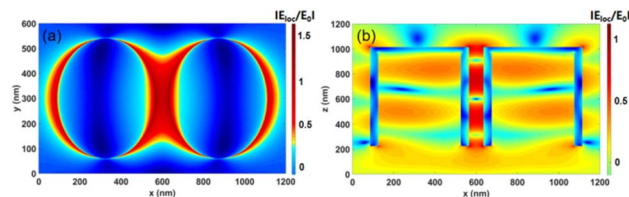


Fig. 8 Intensity distribution of the theoretical electric field: (a) inside the silver nanocolumn array; (b) on the side of the silver nanocolumn array.

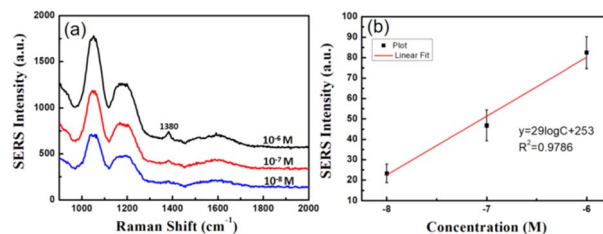


Fig. 9 (a) SERS spectra obtained using evanescent wave fiber SERS probes for thiram aqueous solutions. (b) Linearity analysis of thiram aqueous solutions with concentrations ranging from  $10^{-8}$  to  $10^{-6}$  M.

denotes the amplitude of the input source electric field (with  $E_0$  set to 1 in this case).<sup>27</sup> The calculated EF value was found to be  $1.05 \times 10^6$ . Therefore, the silver nanocolumn array structures proved advantageous for heightening the Raman signal, aligning well with the experimental results.

### 3.4 Applications of evanescent wave fiber SERS probes

From the above analyses, we use the optical fiber probes to verify *in situ*, rapid and highly sensitive SERS detection of thiram. Lake water obtained from a local lake was used as a solvent to prepare the thiram solutions. By dipping the SERS probes into the thiram solutions, Fig. 9(a) shows the *in situ* liquid phase SERS spectra. The main Raman peaks of thiram were observed, and the sensitivity was  $10^{-8}$  M. Fig. 9(b) illustrates the relationship between the normalized SERS intensity at  $1380$  cm $^{-1}$  and the logarithm of thiram concentration ranging from  $10^{-8}$  M to  $10^{-6}$  M. The experimental results show that the evanescent wave fiber SERS probe has high sensitivity in detecting thiram and better linearity ( $R^2 = 0.9786$ ) to thiram, which suggests that it is satisfactory to apply the evanescent wave fiber SERS probes for analyte quantitation. This shows that the evanescent wave fiber SERS probes we fabricated have important applications in monitoring water environments.

## 4. Conclusions

In conclusion, we demonstrated a highly sensitive ECF SERS probe with a silver nanocolumn array. The ECF SERS probe is prepared by first removing the cladding to expose the core and then fabricating silver nanocolumns on the curved surface of the exposed core. The optimized core diameter of the ECF SERS probe is  $36.55$   $\mu\text{m}$  by balance preparation time, transmission



loss and evanescent wave intensity. Such ECF SERS probes can efficiently detect 4-ATP *in situ*, and a low detection limit of  $10^{-10}$  M is achieved. The main reason may originate from the ECF, which can expose the evanescent field to the surrounding silver nanocolumn array. The evanescent field of the ECF boundary is enhanced by silver nanocolumn arrays, which are useful for SERS signal excitation. The ECF SERS probes were demonstrated to be highly sensitive, low cost, and easy to manufacture. Another important aspect was that the experimental results successfully demonstrated that the ECF SERS probe has good selectivity, repeatability and rapid recovery ability. Additionally, the numerical simulation results verify the effectiveness of our proposed scheme. The ECF SERS probe is further adopted to detect pesticide residues in river water, and a detection limit of  $10^{-9}$  M for thiram is obtained. The ECF SERS probe shows the excellent properties of high-sensitive, real-time, remote-sensing, fast-response, and *in situ* detection while possessing the advantages of simplicity, convenience, and low-cost, suggesting large potential in accurate and precise detection in the chemical and environmental safety fields.

## Data availability

The authors confirm that the data supporting the findings of this study are available within the article and its ESI.†

## Conflicts of interest

There are no conflicts to declare.

## Acknowledgements

This work was financially supported by the Natural Science Foundation of China (Grant No. 52071187, 52271133).

## References

- 1 J. Li, Y. Huang, Y. Ding, Z. Yang, S. Li, X. Zhou, F. Fan, W. Zhang, Z. Zhou, D. Wu, B. Ren, Z. Wang and Z. Tian, Shell-isolated nanoparticle enhanced Raman spectroscopy, *Nature*, 2010, **464**, 392–395.
- 2 X. Xu, H. Li, D. Hasan, R. Ruoff, A. Wang and D. Fan, Near-field enhanced plasmonic-magnetic bifunctional nanotubes for single cell bioanalysis, *Adv. Funct. Mater.*, 2013, **23**, 4332–4338.
- 3 X. Zhang, K. Zhang, H. von Bredow, C. Metting, G. Atanasoff, R. Briber and O. Rabin, Remote chemical sensing by SERS with self-assembly plasmonic nanoparticle arrays on a fiber, *Front. Phys.*, 2022, **9**, 752943.
- 4 A. Zrimsek, N. Chiang, M. Mattei, S. Zaleski, M. McAnally, C. Chapman, A. Henry, G. Schatz and R. Van Duyne, Single-molecule chemistry with surface-and tip-enhanced Raman spectroscopy, *Chem. Rev.*, 2016, **117**, 7583–7613.
- 5 H. Wang, E. You, R. Panneerselvam, S. Ding and Z. Tian, Advances of surface-enhanced Raman and IR spectroscopies: from nano/microstructures to macro-optical design, *Light: Sci. Appl.*, 2021, **10**, 161.
- 6 J. Chen, S. Li, F. Yao, *et al.*, Progress of microfluidics combined with SERS technology in the trace detection of harmful substances, *Chemosensors*, 2022, **10**(11), 449.
- 7 E. Smythe, M. Dickey, J. Bao, G. Whitesides and F. Capasso, Optical antenna arrays on a fiber facet for *in situ* surface-enhanced Raman scattering detection, *Nano Lett.*, 2009, **9**, 1132.
- 8 A. Pesapane, A. Lucotti and G. Zerbi, Fiber-optic SERS sensor with optimized geometry: testing and optimization, *J. Raman Spectrosc.*, 2010, **41**, 256.
- 9 T. Vo-Dinh, H. N. Wang and J. Scaffidi, Plasmonic nanoprobe for SERS biosensing and bioimaging, *J. Biophotonics*, 2010, **3**, 89.
- 10 Y. Zhu, R. Dluhy and Y. Zhao, Development of silver nanorod array based fiber optic probes for SERS detection, *Sens. Actuators, B*, 2011, **157**, 42–50.
- 11 P. Pinkhasova, H. Chen, J. Kanka, P. Mergo and H. Du, Nanotag-enabled photonic crystal fiber as quantitative surface-enhanced Raman scattering optofluidic platform, *Appl. Phys. Lett.*, 2015, **106**, 071106.
- 12 Y. Long, H. Li, X. Yang, Y. Yuan and M. Zheng, Controlling silver morphology on a cramped optical fiber facet *via* a PVP-assisted silver mirror reaction for SERS fiber probe fabrication, *New J. Chem.*, 2021, **45**, 4004–4015.
- 13 P. Tao, K. Ge, X. Dai, D. Xue, Y. Luo, S. Dai, T. Xu, T. Jiang and P. Zhang, Fiber optic SERS sensor with silver nanocubes attached based on evanescent wave for detecting pesticide residues, *ACS Appl. Mater. Interfaces*, 2023, **15**, 30998–33100.
- 14 S. J. Weng, L. Pei, J. S. Wang, T. G. Ning and J. Li, High sensitivity D-shaped hole fiber temperature sensor based on surface plasmon resonance with liquid filling, *Photonics Res.*, 2017, **5**, 103.
- 15 F. Chiavaioli, P. Zubiante, I. Del Villar, C. Zamarreno, A. Giannetti, S. Tombelli, C. Trono, F. Arregui, I. Matias and F. Baldini, Femtomolar detection by nanocoated fiber label-free biosensors, *ACS Sens.*, 2018, **3**(5), 936–943.
- 16 T. K. Yadav, R. Narayanaswamy, M. H. Abu Bakar, Y. M. Kamil and M. A. Mahdi, Single mode tapered fiber-optic interferometer based refractive index sensor and its application to protein sensing, *Opt. Express*, 2014, **22**, 22802.
- 17 N. N. Luan, R. Wang, W. H. Lv and J. Q. Yao, Surface plasmon resonance sensor based on D-shaped microstructured optical fiber with hollow core, *Opt. Express*, 2015, **23**, 8576.
- 18 T. Y. Huang, Highly sensitive SPR sensor based on D-shaped photonic crystal fiber coated with indium tin oxide at near-infrared wavelength, *Plasmonics*, 2016, **12**, 583.
- 19 A. Van Brakel, C. Grivas, M. N. Petrovich and D. J. Richardson, Photonic bandgap fiber optical correlation spectroscopy gas sensor, *Opt. Express*, 2007, **15**, 8731.
- 20 C. Martelli, P. Olivero, J. Canning, N. Grothoff, B. Gibson and S. Huntington, Micromachining structured optical fibers using focused ion beam milling, *Opt. Lett.*, 2007, **32**, 1575.



- 21 S. C. Warren-Smith, H. Ebendorff-Heidepriem, T. C. Foo, R. Moore, C. Davis and T. M. Monro, Exposed-core microstructured optical fibers for real-time fluorescence sensing, *Opt. Express*, 2009, **17**, 18533.
- 22 Y. Wu, X. Deng, F. Li and X. Zhuang, Less-mode optic fiber evanescent wave absorbing sensor: Parameter design for high sensitivity liquid detection, *Sens. Actuators, B*, 2007, **122**, 127.
- 23 L. Meng, L. Shang, S. Feng, Z. Tang, C. Bi, H. Zhao and G. Liu, Fabrication of a three-dimensional (3D) SERS fiber probe and application of *in situ* detection, *Opt. Express*, 2022, **30**, 2353.
- 24 Y. Zhang, C. Gu, A. M. Schwartzberg and J. Z. Zhang, Surface-enhanced Raman scattering sensor based on D-shaped fiber, *Appl. Phys. Lett.*, 2005, **87**, 123105.
- 25 F. Chiavaioli, P. Zubiato, I. Del Villar, C. R. Zamarreno, A. Giannetti, S. Tombelli, C. Trono, F. J. Arregui, I. R. Matias and F. Baldini, Femtomolar detection by nanocoated fiber label-free biosensors, *ACS Sens.*, 2018, **3**, 936.
- 26 R. Chu, C. Guan, J. Yang, Z. Zhu, P. Li, J. Shi, P. Tian, L. Yuan and G. Brambilla, High extinction ratio D-shaped fiber polarizers coated by a double graphene/PMMA stack, *Opt. Express*, 2017, **25**, 13278.
- 27 P. Stiles, J. Dieringer, N. Shah and R. Van Duyne, Surface-enhanced Raman spectroscopy, *Annu. Rev. Anal. Chem.*, 2008, **1**, 601.

